



1 **Rising bubbles as mechanism for scavenging and aerosolization of diatoms**

2

3 **Roman Marks¹, Ewa Górecka² Kevin Mc Cartney³, Wojciech Borkowski¹**

4

5 ¹University of Szczecin, Faculty of Geosciences, Physical Oceanography Unit,
6 Mickiewicza 16, 70-383 Szczecin, Poland;

7 ²Natural Sciences Education and Research Centre, University of Szczecin,
8 Palaeoceanology Unit, Mickiewicza 16a, 70-383 Szczecin, Poland;

9 ³Department of Environmental Sciences and Sustainability, University of Maine at Presque
10 Isle, Presque Isle, ME 04769, USA.

11

12 *Correspondence to:* Roman Marks (Roman.Marks@usz.edu.pl)

13

14 **Abstract.** Bubbles rising in clean saline water cause steady displacement of ions at the bubble
15 boundaries that separate anions and cations based on ion mass. Anions of greater mass are
16 resistant to displacement and concentrate on the bubble upper half sphere, while smaller and
17 less massive cations are displaced towards lower pressure of the bottom half sphere. The
18 separation into anionic and cationic domains on the bubble curvatures creates electric polarity
19 that may draw particulates dispersed in the water. Viable diatoms as well as bacteria develop
20 negative charge on outer membranes, that are attracted to the cationic bubble bottom half
21 sphere and pocket. When bubble bursts at the air/water interface the diatoms and bacteria are
22 ejected into the air with initial or secondary jet droplets that are projected upward with a small
23 water column derived from a cationic vortex. Experiments conducted in brackish and oceanic
24 saline water on *Nanofrustulum* and *Cyclotella cells* indicated that the averaged concentration
25 in jet droplets compared to the original water volume (here termed the enrichment factor) for
26 aerosolized diatoms may range from 8 to 307.

27

28 **1 Introduction**

29 **1.1 Rising bubbles**

30 Bubbles in the ocean are abundantly caused by breaking waves in surface waters (Woodcock,
31 1953; Blanchard and Syzdek, 1970; Monahan et al., 1983; Garbalewski and Marks, 1987;
32 Czerski et al., 2011) and rain drop impact upon the water surface (Blanchard and Woodcock,
33 1957; Marks, 1990). Bubble plumes are diffused by near surface turbulence to depths of four
34 to six times the significant wave height (Thorpe, 2001). Production of bubbles increases with
35 wind speed (Blanchard, 1963; Monahan et al., 1983; Callaghan et al., 2007) and effervescence
36 bubbles increase with dissolved gas supersaturation (Stramska et al., 1990; Marks, 2008)
37 which is common in shallow water environments, especially, when phytoplankton production



38 of oxygen occurs during spring warming and upwelling (Blanchard, 1963; Garbalewski and
39 Marks, 1987). Under such conditions enhanced formation of small bubbles and sea-derived
40 aerosols may occur (Garbalewski and Marks, 1987; Stramska et al., 1990; Marks, 2008).

41 Bubbles produced by breaking waves in oceanic water range from radius 1 to several
42 thousand μm with maximum occurrence about 25 μm (Woolf, 1997). Although wave break
43 agitation is the main mechanism of bubble generation in fresh and oceanic waters, only saline
44 waters generate abundant small bubbles (Thorpe, 2001; Woolf, 1997; Czerski et al., 2011).
45 Recent research indicates that small bubbles with radii less than 30 μm are especially
46 abundant and have significant effect on upper ocean optical properties (Stramski and
47 Tęgowski 2001; Czerski et al., 2011). A typical breaking wave generates a downward
48 circulating rotor-like motion reaching a depth equal to the wave height. Thus a surface wave
49 of 1 m height, generated at wind velocity 8 m/s, can produce and disperse bubbles to about 1
50 m water depth (Thorpe, 2001) while during rain bubbles may occur to about 10-20 cm depth
51 (Blanchard, 1963; Katsaros and Buettner, 1969). However, local generation of splash droplets
52 and bubbles is further enhanced during high and in particular tropical precipitation
53 (Garbalewski and Marks, 1987). Higher water temperature decreases water viscosity (Woolf,
54 1997) which enhances bubbles and sea salt aerosol production.

55 After downward dispersion in the water column, bubbles tend to surface according to
56 bubble volume that controls buoyant vertical motion, and gradually grow in size, especially
57 under the condition of dissolved gases supersaturation (Woolf, 1997; Marks, 2008). Field and
58 laboratory experiments confirm that bubble production in oceanic water and generation of sea
59 salt aerosols increases with increasing degree of dissolved gases saturation (Stramska et al.,
60 1990; Marks, 2008). In addition, bubble production increases with water temperature and
61 water to air thermal gradient (Marks, 1987).

62 Experiments on the rotational features of a rising bubble (Marks, 2014) suggest that
63 interaction with ions in “clean or relatively clean” sea water can separate cations and anions
64 into charge polarized and oppositely rotating domains. The principle on which ions are
65 separated by rising bubbles is based on mass differences between the main ionic hydrates (Cl^-
66 and Na^+) that compose sea water. Using a Cl/Na atomic mass equal to 1.542 (Kropman and
67 Bakker, 2001) the bubble mediated selection of ions that collide with bubble outer curvatures
68 may be based on ionic hydrate mass differences. Anionic hydrates are more resistant to
69 displacement and concentrate on the upper bubble half sphere, while lighter and smaller
70 cationic hydrates are drawn to a low pressure area, associated with the bubble bottom half
71 sphere and sub-bubble vortex (Marks, 2014; 2015). Ionic motion accelerated at the moment of



72 interception with a bubble boundary may exceed 10 times the gravitational acceleration,
73 which generates opposite directed rotations, anionic-dextrorotary (a-dx) on the bubble upper
74 curvature and cationic-levorotary (c-lv) on the bubble bottom half sphere (Marks, 2014).

75

76 1.2 Bubble mediated scavenging of bio-cells

77 First evidences of bubble mediated bio-cells scavenge and incorporated into jet droplets was
78 reported by Blanchard and Syzdek (1970), who investigated the aerosolization of bacteria
79 *Serratia marcescens* by uniform - sized bubbles in water columns of different heights. The
80 bacteria were collected and incubated on agar plates and counted. The number of bacteria
81 cells ejected with jet droplets (N_{jd}) rated to bacteria concentration in the same (as in droplets)
82 volume of water in which the bubbles rise/burst (N_w) was used to estimate the “enrichment
83 factor- (E_f)” in a form:

$$84 \quad E_f = N_{jd} / N_w. \quad (1)$$

85 Blanchard and Syzdek (1982) determined E_f values up to 600, in experiments were the
86 bubble rise distance in the water column was 10 cm. More recent experiments reported that
87 (E_f) values of bacteria in aerosol droplets range from one order of magnitude for oceanic
88 waters (experiments conducted by Aller et al., 2005) to three orders for brackish coastal
89 waters (Marks et al., 2001). Moreover, the experiments indicated that the sea - derived
90 droplets may also contain a significant share of fungi (Marks et al., 2001) and viruses
91 (Matthais-Maser and Jaenicke, 1994; Aller et al., 2005; Burrows et al., 2009). However, a
92 high discrepancy between level of airborne bacteria was reported by Mayol (2014) likely
93 associated with the method applied to bacteria counting. A modern method based on
94 RNA/DNA identification offers significantly higher counts that include both viable and dead
95 cells, while previous traditional methods counted only viable cells.

96 The waterborne bacteria may effectively adhere to the bubble boundary (Blanchard
97 and Syzdek, 1982; Weber et al., 1983). Both teams of researchers reasoned that interception
98 occurs when small particles move along fluid streamlines around the bubble wall, thus
99 particles (including bacteria) are accumulated at the bubble boundary. With increasing
100 distance of rise the bubble surface changes gradually from a mobile to rigid structure, which
101 decreases the rate of bacteria collection (Weber et al., 1983).

102 Until now no bubble related research has focused on diatom scavenge. Nevertheless,
103 airborne transport of both freshwater and marine diatom taxa was documented in various



104 locations including a highly elevated glaciers (Sherilyn et al., 2015) and continental interiors
105 such as the Antarctic continent (Budgeon et al., 2012; Stanish et al., 2013). Thus, one
106 purpose for this study was to collect experimental evidences that diatom cells may be
107 scavenged and aerosolized.

108

109 **1.3 Bubbles burst at water-air interface**

110 At a clean air-water interface, bubbles of diameter (D) burst almost instantly upon arrival and
111 eject a few large jet droplets of diameter that is roughly an order of magnitude less than D .
112 The droplets are derived from the bubble lower half and hundreds of smaller film droplets
113 derived from upper half-bubble (Blanchard and Woodcock, 1957; Lovett, 1978; Blanchard,
114 1989). Sea-derived droplets supply the troposphere with various materials dominated by sea
115 salt aerosols that provide condensation nuclei and affect electric properties (Blanchard, 1963;
116 Marks, 1990). In addition, marine aerosols contain a significant share of trace elements and
117 hydrophobic particulates (Liss, 1983; Novakov and Penner, 1993; Duce, 2001; Tuck, 2002;
118 Bigg and Leck, 2008; Marks and Beldowska 2001).

119 About 50% of kinetic wave energy imparted into ocean wave motions is dissipated by
120 bubbles (Terray et al., 1996). The bubble motions including the rotational kinetics (Marks,
121 2014; 2015) play a significant role in redistribution of radiant solar energy absorbed by the
122 near surface water. The energy dissipation continues from the moment of bubble formation in
123 the water column and after the bubble bursts at the sea surface, where a share of rotational
124 kinetic energy is transferred into jet droplets (Marks, 2014). After this process, a final
125 dissipation of energy to heat and evaporation occurs with duration according to evaporation
126 rate and air relative humidity, which over the sea is usually higher than 80%, allowing
127 droplets to persist in the liquid phase (Garbalewski and Marks, 1987). With respect to the
128 humidity, oceanic tropical belt and warm compartments near the east coast of continents are
129 the most efficient evaporative zones on the Earth (Yu, 2007).

130 Saline waters can generate bubbles and aerosols which could supply the troposphere
131 with abundant bio-aerosols (Burrows et al., 2009). Laboratory experiments by Blanchard and
132 Syzdek (1970), Weber et al. (1983) and Marks et al. (2001) indicated that jet droplets may be
133 highly enriched by bacteria. The ratio of bacteria in the jet droplets to that in the bulk water
134 varies with the rise distance in the water column and is highest during the first few up to c. 30
135 cm of rise (Weber et al., 1983) then decreases due to overload with respect to scavenged
136 cargo (Blanchard and Syzdek, 1970; Marks et al., 2001). The present research further explores



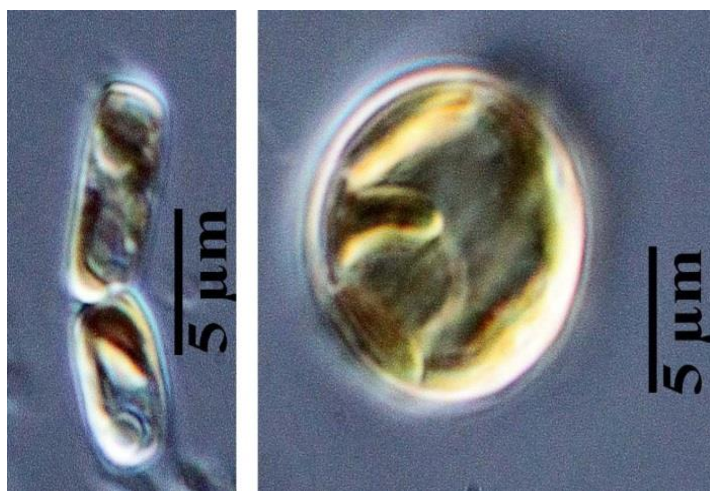
137 the bubble mediated scavenge and aerosolization of bio-molecules with special attention
138 given to diatoms.

139

140 2 Methods

141

142 Diatoms stains were obtained from Szczecin Diatom Culture Collection (SZCZ) curated at the
143 Natural Sciences Education and Research Centre, Faculty of Geosciences, University of
144 Szczecin. Two stains of diatoms were prepared: (1) *Nanofrustulum* sp. (SZCZ_E_517)
145 forming elongated chains of about 3 by 12 μm sizes in two concentration of 11000 and 480000
146 cells / 1 ml suspended in an artificial (f/2) medium of 35 g/kg salinity and (2) *Cyclotella* cf.
147 *meneghiniana* Kützing (SZCZ_E_684) with spherical shape of 10 μm diameter (Fig. 1) in
148 concentration of 3000 cells/1 ml, suspended in artificial (f/2) medium of 15 g/kg salinity. To
149 prepare the solutions an instant sea salt was used.



150

151 **Figure 1.** Stains of diatoms used in experiments: A) elongated *Nanofrustulum* and B)
152 spherical *Cyclotella*. Picture taken by Canon DS 500D using Zeiss Scope A1 with PlanApo
153 x100 lens.

154

155 Experiments were conducted in several stages: 1) an experimental set-up was tested
156 and size of bubbles produced by glass capillary aerator was measured; 2) the bubble-mediated
157 aerosolization of elongated *Nanofrustulum* and spherical *Cyclotella* diatom cells was
158 confirmed; 3) four sets of experiments using the two different diatom stains suspended in
159 brackish and oceanic water were conducted and evaluated; 4) twenty additional experiments
160 were conducted using more concentrated diatom stain suspended in water of 35 b/kg salinity.



161 In addition, complementary investigations were conducted on: 1) the electric charge
162 distribution along the bubble boundaries; 2) charge of jet droplets; 3) outer charge
163 incorporated to diatom membranes; 4) the ejection height of initial and secondary droplets
164 above water level; and 5) diatoms content in initial and secondary jet droplets using
165 negatively charged, vertically placed Plexiglas plate.

166

167 2.1 Experimental procedure

168

169 During experiments 150 ml volume of each prepared suspension was placed in a 200 ml glass
170 beaker and aerated using a glass capillary, producing stream of bubbles diameter $D = 1.2$ mm.
171 Bubbles were generated by air pump equipped with cotton filter and rose through a 10 cm
172 water column in a 200 ml breaker (Fig. 2). Upon arrival at the water surface a bursting bubble
173 produced 5 to 7 jet droplets, which were collected on a standard microscopy glass slide (26 x
174 76 mm) placed transversely to jet droplet motion at 4 cm above the water surface.

175

176

177

178

179

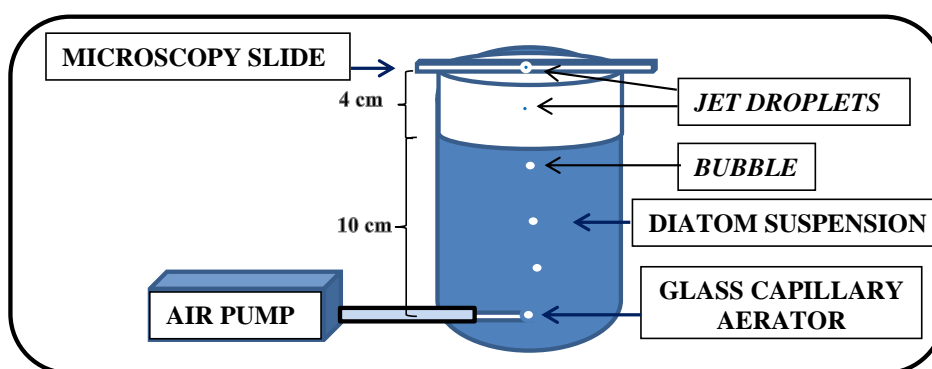
180

181

182

183

184



185

Figure 2. Experimental set-up used to determinate enrichment factor for aerosolized diatoms.

186

187

188

189

190

191

192

193

194

After 2-3 seconds of exposure microscopy slides were placed into Petri dish containing a small volume of distilled water and covered to prevent drying. Counting of diatom cells was conducted using Nikon Eclipse TS100 inverted light microscope with 20X lens. Taking into account that both diatoms concentrations in the water suspension and water salinity (or more precisely the availability of cations) decrease during aeration, only 8 samples were collected to estimate enrichment factor for aerosolized *Cyclotella* diatoms from one suspension of low or moderate concentrated diatom cells. In case of high diatom concentration of *Nanofrustulum* in 35 g/kg salinity, the number of samples was extended to



195 20. However, after analyzing that set of data we noticed that the efficiency of diatom
196 aerosolization increased, indicating that rising bubbles reduced concentrations of diatoms
197 (solution was gradually cleaned) during the experiments.

198 In order to detect electric charge distribution around the rising bubble boundaries an
199 oscilloscope, type HANTEK®-DS01201BV was used, allowing to trace the voltage polarity
200 in mV with 0.1 mV detection limit and 0.5% accuracy. Similarly, the electric charge of
201 diatoms adhered onto the oscilloscope probe was measured. The complementary observations
202 allowed determination of ion accumulation and electric polarity on both bubble curvatures
203 and diatom exteriors. The presence of diatoms included in both the initial and secondary jet
204 droplets was investigated by microscopy glass plates exposed at different heights above water
205 level. In addition, a deflection of jet droplets towards negatively charged Plexiglas plate (24 x
206 6 x 2 mm) was observed.

207

208 3 Results

209 3.1 Aerosolization of diatom stains

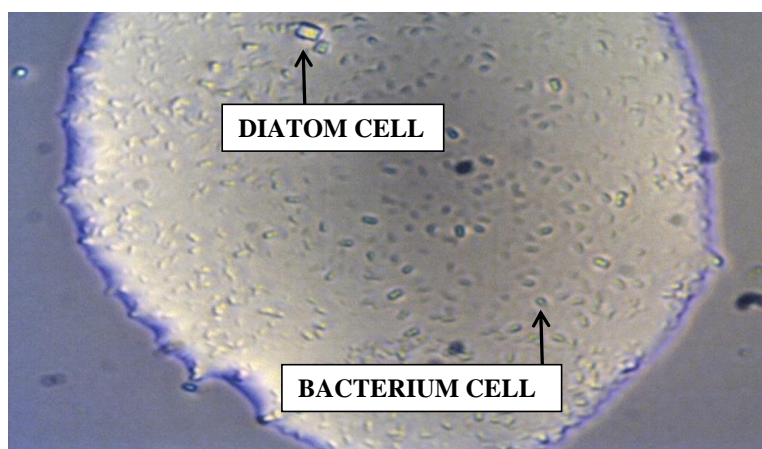
210

211 A single burst of bubble $D = 1.2$ mm may ejects about 4-8 droplets from a clean water at
212 temperature (T_w) of 20°C (Blanchard and Syzdek, 1982); the number of jet droplets that
213 contained diatoms were counted and compared with droplets that lacked diatom cargo.
214 Conducted screening showed that only 20-25% of jet droplets were enriched by diatoms,
215 which suggests that the process of diatom aerosolization might be influenced by a
216 combination of factors operative in the water column, or at air-water interface. To explore
217 these variables a set of experiments collected droplets at different elevations above water level
218 to determinate whether diatoms were included in the initial large jet droplets or secondary
219 droplets. The observations indicated that not exclusively top jet droplets were enriched by
220 diatoms. That result suggests that perhaps a first initial droplets are projected upward too fast
221 to skim diatoms thus the next and slower droplet that follows, hereafter called sub - initial
222 droplet may lift diatoms.

223 An example of a jet droplet containing diatoms and bacteria is illustrated in Fig. 3,
224 which shows the initial or sub-initial jet droplet of about $d = 0.12$ mm, ejected by bubble of c.
225 $D = 1.2$ mm, at $T_w = 22.1^\circ\text{C}$. A cargo of diatom cells in all collected initial jet droplets ranged
226 from 1-12 for *Nanofrustulum* and 1-3 for *Cyclotella* stains indicating that elongated
227 (*Nanofrustulum*) diatoms that offer 8% greater outer surface were subject to more enhanced
228 scavenge as compared with spherical (*Cyclotella*) cells. In the case of *Nanofrustulum*



229 aerosolization, the higher salinity of 35 g/kg might contribute to enhanced scavenge and
230 aerosolization, since initial jet drops are ejected higher above seawater than above distilled
231 water (Blanchard, 1989). Since diatom cells are relatively large, as compared with bacteria
232 cells, these should require more energy for ejection into air.



233
234 **Figure 3.** An example of bio-cargo incorporated into the jet droplet. Image taken with Zeiss
235 AxioCam ERc5s using Nikon Eclipse TS100 with 20X lens.
236

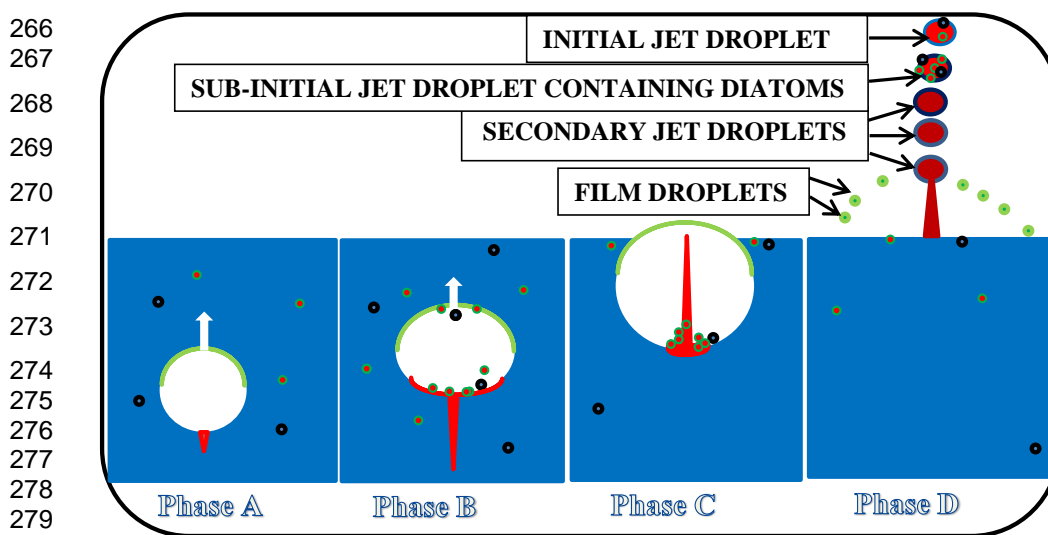
237 Bubbles rising in more concentrated diatom suspensions produced fewer jet droplets,
238 only ~5 from a diatom suspension of 11000 cells / ml, as compared with ~7 jet droplets
239 ejected from suspension of 3000 cells / ml (Table 1). This result indicates that the rising
240 bubble has a limited ability to collect diatom cells. Steadily accumulated bio-cargo reduces
241 also the speed of bubble rise and in turn decreases the energy available for upward projection
242 of bottom bubble vortex (see Fig. 4, Phase B). That is consistent with observations reported
243 by (Woolf and Thorpe, 1991), who observed that overloaded, so called “dirty bubbles” of 0.2
244 mm diameter rises with velocity of 0.6 cm/s as compared with “clean bubbles” of the same
245 diameter that surface with velocity 2.1 cm/s. A similar result was reported by Marks et al.
246 (2001) and showed that aerosolization of bacteria from polluted coastal sea water was
247 suppressed.

248 The rising bubble and induced diatom scavenge and related aerosolization is shown in
249 Figure 4. Four phases may be distinguished: separation of ions into cations and anions (Phase
250 A); scavenge of negatively charged cells from the water column (Phase B); sudden bubble
251 stop at the water/air interface and projection of cationic jet column that skims negatively
252 charged cells (Phase C); ejection of one jet droplet that contains diatoms and several without
253 bio-cargo along with spread of film droplets (Phase D). Distinction between the initial jet



254 droplets and secondary droplets were done by considering ejection heights according to
255 (Blanchard and Syzdek, 1982; Blanchard, 1989). During the experiments ejection height of
256 initial jet droplets was about 16-18 cm, while the secondary jet droplets were typically
257 projected to 3-12 cm (Table 1).

258 The enrichment factor, calculated as the number of diatoms included in the initial or
259 sub-initial jet droplet of volume $9.05 \cdot 10^{-6}$ ml divided by the number of diatoms suspended in
260 solution, indicated that diatoms incorporated into enriched jet droplets were directly derived
261 from the bubble bottom layer. Considering that the initial jet droplets also contains an
262 enhanced share of positively charged cations the process of diatom scavenge in the water
263 column and related ejection into air may operate on the electrostatic (cationic) adhesion of
264 negatively charged diatoms. Thus when bubble burst at the air-water interface diatoms could
265 be accommodated to a bit slowed (sub-initial) droplet (Fig. 4).



281 **Figure 4.** Four phases of a rising bubble mediated scavenging of bio-cells and related
282 aerosolization from: initial stage of developing upper anionic domain (marked by grey) and
283 bottom cationic vortex (marked by black) (Phase A); followed by cationic attraction and
284 scavenging of negative charged cells (Phase B); via projection of cationic jet, skimming
285 collected bio-cells (Phase C); to final ejection of initial and sub-initial jet droplets with bio-
286 cargo and secondary jet droplets along with spread of film droplets into the air (Phase D).
287

288 Assembled details regarding experimental conditions, including diatom shape, cell
289 concentrations, water temperature, salinity and estimated E_f for both investigated diatom
290 stains are listed in Table 1. These observations relate to the bubble-mediated diatoms
291 scavenging suspended in two samples of different salinities, that are typical for brackish 15 g/kg and



292 oceanic 35 g/kg salinities. Therefore the diatom stains were prepared to obtain typical natural
 293 concentrations of diatom in sea water. The experiments were performed in solutions
 294 containing 11000 *Nanofrustulum* and 3000 of *Cyclotella* cells in 1 ml volume.

295

296 **Table 1.** Data set describing laboratory experiment evaluating diatoms aerosolization.

297

298 MEDIUM/parameter	<i>Nanofrustulum</i>	<i>Cyclotella</i>
299 DIATOMS/		
300 concentration (1 ml)	11000	3000
301 shape	elongated	spherical
302 size (μm)	$\sim 3 \times 12$	~ 10
303 detected charge on outer	negative	negative
304 BUBBLE/		
305 (<i>D</i>) diameter (mm)	1.2	1.2
306 volume (ml)	$\sim 0.905 \cdot 10^{-3}$	$\sim 0.905 \cdot 10^{-3}$
307 detected charge (vortex)	positive (strong)	positive (strong)
308 detected charge (upper)	negative (weak)	negative (weak)
309 rise distance (mm)	~ 100	~ 100
310 ENRICHED INITIAL OR SUB-INITIAL JET DROPLET/		
311 (<i>d</i>) diameter (mm)	~ 0.12	~ 0.12
312 volume (ml)	$\sim 0.905 \cdot 10^{-6}$	$\sim 0.905 \cdot 10^{-6}$
313 ejection height (cm)	12-16	12-16
314 detected charge	positive (strong)	positive (strong)
315 number of diatoms in enriched droplets	1-12	1-3
316 (<i>E_f</i>) enrichment factor	370 (averaged)	101 (averaged)
317 SECONDARY JET DROPLETS/		
318 (<i>d</i>) diameter (mm)	~ 0.12	~ 0.12
319 volume (ml)	$\sim 0.905 \cdot 10^{-6}$	$\sim 0.905 \cdot 10^{-6}$
320 ejection height (cm)	3-12	3-12
321 number of droplets	4	6
322 detected charge	positive (weak)	positive (weak)
323 (<i>E_f</i>) enrichment factor	0	0
324 WATER SOLUTION/		
325 (<i>T_w</i>) temperature ($^{\circ}\text{C}$)	22.1	22.1
326 (<i>S</i>) salinity (g/kg)	35	15

327

328 After experiments with diatom aerosolization from moderate concentrated suspension
 329 of 11000 *Nanofrustulum* cells in 1 ml a next set with significantly concentrated medium of
 330 840000 cells / 1 ml was completed. The conditions simulate a diatom bloom and refer to
 331 salinity 35 g/kg. Obtained results showed much lower *E_f* values that ranged from ~ 5 to 30 and
 332 steadily increased during the elapsed time of experiment. The averaged value of *E_f* calculated
 333 from all 20 samples was ~ 8 (Table 2).

334

335 Both experiments indicated that the averaged values of *E_f* estimated for diatoms
 aerosolized from relatively low concentrated suspension was 101 for spherically shaped



336 *Cyclotella* cells and 307 for elongated *Nanofrustulum* cells (Table 1). However, the *Ef*
337 significantly dropped to 8 when *Nanofrustulum* cells were aerosolized from more
338 concentrated suspension (Table 2).

339

340 **Table 2.** Enrichment factor for *Nanofrustulum* aerosolized by uniform bubbles of $D=1.2$ mm
341 rising in water suspension of 35 g/kg salinity for distinctly different diatom concentrations.

342

343 **Parameter**

344

345 Concentration (1 ml)	11000	840000
346 number of diatoms in enriched droplets	1-12	1-23
347 (<i>Ef</i>) enrichment factor	370 (averaged)	8 (averaged)
348 (<i>T_w</i>) water temperature (°C)	22.1	22.1
349 (<i>S</i>) water salinity (g/kg)	35	35

350

351

352 **4 Discussion**

353

354 The collected evidences suggests that the bubble-mediated mechanism of diatom scavenge in
355 the water column and enrichment in aerosol droplets may depend on a combination of factors,
356 controlled by the positively charged (cationic) sub-bubble vortex (Marks, 2014) that attracts
357 negatively charged diatoms in the water. The sub-bubble vortex gathers rotational momentum
358 during the bubble rise in the water column and projects a small whirling water jet producing a
359 few jet droplets (Blanchard and Woodcock, 1957). If that concept is correct, the enrichment
360 factors of aerosolized diatoms and bio-cells may depend on the strength of bottom bubble
361 cationic vortex that forms a rotating pocket as well as the negative charge imparted to the
362 diatoms (this paper) or bacteria outer membranes (Blanchard and Syzdek, 1978; 1982; Weber
363 et al., 1983; Marks et al., 2001; Aller et al., 2005; Mayol et al., 2014).

364 The diatom uplift may be reduced as compared with bacteria (Blanchard and Syzdek,
365 1978) due to the higher weight of diatom cells. Thus the accommodation of diatoms into sub-
366 initial droplets derived from the water jet/column is more probable as depicted in Figure 4,
367 Phase C. Diatoms as relatively large objects suspended in the water thus are more resistant to
368 bubble-mediated drawing and related aerosolization, as compared with bacteria.

369 Extended laboratory experiment reported by Blanchard and Syzdek (1970) evaluated
370 the enrichment factor *Ef* of bacteria *Serratia marcescens* ejected with the initial jet droplets,
371 which exceeded 600, when the rise distance of bubbles through the bacteria suspension was c.
372 10 cm. Later, (Blanchard and Syzdek, 1978) determined that the concentration of bacteria is
373 always highest in the initial jet droplet and decreases progressively in the lower drops, being



374 lowest in the last ejected droplet. That however was not the case with ejection of diatoms.
375 Thus, at this stage of research we may only state that a single bubble at the moment of burst
376 projects diatoms which are incorporated to one of five-seven jet droplets.

377 The averaged values of E_f estimated for spherical *Cyclotella* cells was about 3-4 times
378 lower than that for the elongated *Nanofrustulum* cells. This indicates that the elongated cells
379 may integrate more negative anions on more expanded outer membranes, and these are more
380 effectively scavenged and aerosolized by bubbles. The E_f values obtained for diatoms exceed
381 two orders of magnitude the original concentrations in water suspensions, which indicate that
382 even relatively large and heavy diatoms, as compared with bacteria, are scavenged by rising
383 bubbles and aerosolized. Note that E_f values obtained in our laboratory study for aerosolized
384 diatoms are about 1-2 orders of magnitude lower than that obtained for bacteria (Blanchard
385 and Syzdek 1978; 1979; Marks et al., 2001; Mayol et al., 2014). However the values of E_f
386 decreased to 8 for the more concentrated suspension show that the efficiency of bubble-
387 mediated cells scavenge and aerosolization decreases with increasing content of cells
388 dispersed in the water. The range of E_f values obtained for diatoms is consistent with that
389 obtained for bacteria aerosolized from polluted sea reported by Marks et al. (2001).

390 The expanded interfacial of diatom cells, may accommodate relatively more negative
391 charge and contribute to enhanced cationic charge induced attraction of diatoms to the rising
392 bubbles. In contrast, the bacteria in aquatic systems are much smaller and more abundant, thus
393 bacterial concentrations in aerosols and sea surface microlayer are typically significantly
394 higher (Aller et al., 2005; Mayol et al., 2014) as compared with diatoms. However, the
395 charge around (in the outer membranes) and inside (most likely centered in the RNA/DNA
396 nucleus) the diatoms and bacteria cells implies that the cationic electrostriction is a key
397 enforcing factor on the overall distribution of electric charge in bio-cells.

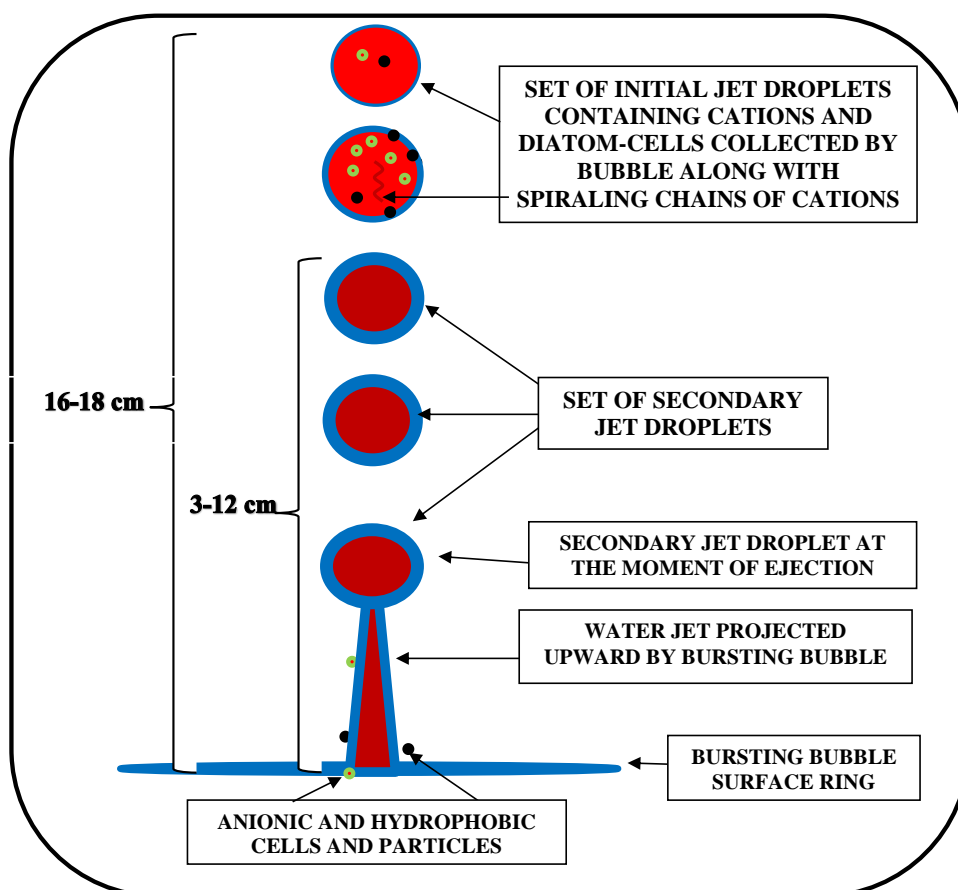
398 The complementary experiments using a negatively charged Plexiglas exposed near
399 the place of bubble burst allowed observation of the trajectory of jet droplets which indicated
400 that all jet droplets carry strong cationic loads. These observations also indicate that both
401 initial and sub-initial jet droplets were somehow more vigorously deflected towards
402 negatively charged Plexiglas plate as compared with secondary jet droplets (see Fig. 5).

403 Intriguing is also that enriched initial jet droplets, beside the condensed bio-cargo, also
404 incorporate a load of spiraling chains of cations (Marks, 2015). Observations indicate that
405 cations are gaining rotational energy under the pirouette narrowing of motion proceeded
406 within the sub-bubble vortex (Marks, 2015). That accelerated motion is then projected upward
407 when bubble bursts at the water surface and share of rotational energy may later contribute to



408 creation and accumulation of RNA/DNA inside airborne droplets (Marks, 2015). In addition,
409 the highly energetic cationic vorticity may permeate into just collected bacteria or diatom
410 cells, trapped inside bio-droplet, as generally illustrated in Figure 5.

411
412
413
414
415
416
417
418
419
420
421
422
423
424
425
426
427
428
429
430
431
432
433



434
435
436
437
438
439
440
441

Figure 5. Illustration of initial and secondary droplets ejecta that results from bubble burst at the water surface (see Fig. 4, Phase D) projecting jet droplets including cationic initial jet droplets skimming negatively charged diatoms.

442 Distinction between the initial and secondary jet droplets were done by considering
443 ejection heights according to Blanchard and Syzdek (1982). During experiments in the present
444 study, the ejection height of initial jet droplets was about 16-18 cm, while the secondary
445 droplets were typically projected to 3-12 cm (Table 1, Fig. 5).

446 Qualitative measurements of electric charge fluctuations accumulated on the rising
447 bubble outer (Table 1) conducted by using oscilloscope indicated a high fluctuation of charge
448 between bulk water and bubble boundaries, when bubble collided with probe head placed at



449 water surface. The charge polarity, indicated positive impulses that were roughly about 4
450 times stronger (due to converging thus more condensed cationic domains) compared to the
451 negative impulses due to diverging thus less condensed anionic domains as illustrated in Fig. 6.
452 In addition, the negative net charge of *Nanofrustulum* community (Table 1) adhered into the
453 oscilloscope probe was confirmed.

454 Collected evidences shows that the cation-mediated electrostriction plays a principal
455 role in bubble vorticity and related attraction/scavenge of bacteria and diatoms by bubbles
456 (Marks, 2014). The efficiency of diatoms scavenge may also depend on anionic charge
457 gathered on outer membranes (Gottenbos et al., 2001) which may depend on more individual
458 bio-cell properties, perhaps related to the charge incorporated into RNA/DNA nucleus. A
459 similar process of cation-induced gathering of anions may stimulate development of negative
460 outer membrane in bacteria (Gottenbos et al., 2001).

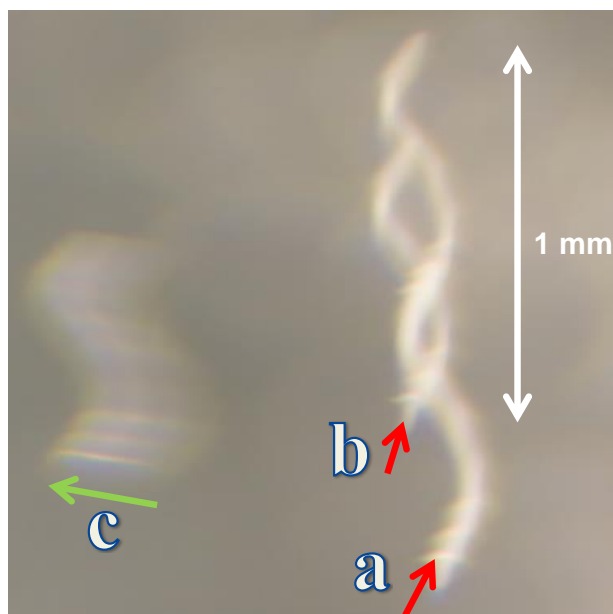
461 In order to underline the rising bubble-induced cationic dominance, one photographic
462 image, taken during the experiment tracing bubble rotary motion in a clean (filtrated) sea
463 water temperature of 38.0°C is shown in Figure 6. The image shows three tracers, two of
464 which (a and b) depict fast rising bubbles sustaining only the sub-bubble cationic rotaries
465 (presumably the anionic rotary was transferred off the bubble). The captured moment, shows
466 two sub-bubble cationic rotaries that interact with each other. A longer tracer of faster rising
467 bubble (a) is passing a slower tracer (b). Both tracers show levorotary spiraling in upward
468 directed motion. The captured tracers deflects each other due to the cationic electric charge, to
469 prevent otherwise inevitable coalescence. In addition, a sinistral (counterclockwise) whirling
470 of both upward directed tracers is visible revealing a strong, converging sub-bubble cationic
471 motion (Fig. 6). To contrast that rather unusual case also a more typical rising bubble tracer
472 (c) is shown revealing a case when both anionic and cationic vorticities are sustained around
473 the bubble, see tracer (c) in Fig. 6.

474 The illustrated case shows that bubbles in clean and warm sea water may rise
475 relatively faster (Fig. 6, tracers a and b). Thus, such rising bubbles may disperse the anionic
476 rotary outward, and the internal cationic vorticity can be visible. The photograph reveals that
477 convergence and related lining-up of cations, ongoing in the rising sub-bubble wake is a
478 dominating rotational feature, while the anionic rotary is weaker, perhaps aligned feature.

479 In open water, which contains substantial loads of suspended matter (including viable
480 bacteria and diatoms) the bubble rotational features may be altered. The velocity of bubble
481 rise may be reduced depending on the quantity and size of particulates collected by bubbles.



482 From time to time, bubbles may become overloaded with respect of collected cargo that may
483 be shed and disintegrate upper and bottom bubble rotaries.
484



485
486

487 **Figure 6.** Rising bubble cationic-rotary tracers (a, b) and anionic/cationic tracer (c) assembled
488 in filtrated, clean sea water taken from Pomeranian Bay at $T_w = 38.0^\circ\text{C}$ and $S = 8 \text{ g/kg}$.
489 Bubbles were produced in laboratory conditions by fuzzy salt (Sal EMS Factitium); image
490 was taken by Tamron Xr Di 28-75 mm lens with reverse ring in 1/10 s time.

491

492 The outlined cationic mechanism seem to play a principal role in organizing motion of
493 ions around bubbles in saline water. The mechanism include also a steady assembly of
494 rotating cations that are ejected into the droplets enriched by preselected biota. Thus the same
495 (coherent) bubble-cationic-rotational processing of matter ongoing in the ocean may assemble
496 coherent bio-active (cation-active) molecules that formed diverse biota.

497

498 5 Conclusions

499

500 Experiments show that rising bubbles in saline water can develop a strong cationic vortex that
501 scavenge diatoms in water, which are transported to the surface and eject as jet droplets into
502 air. The mechanism operates on cationic principles that include:

503

- 504 1) effective cationic-mediated scavenge of negatively charged diatoms that are collected in large numbers during bubble rise in the water column,



505 2) diatoms are collected and concentrated in rotating bubble bottom pocket,
506 3) diatoms are aerosolized in sub-initial jet droplets when bubble bursts.
507 The enrichment factor for aerosolized diatoms strongly decreases with increasing
508 concentration of suspended matter in the water column.

509 In addition, experiments indicate that the cationic selection of diatoms depend on the
510 cells outer negative charge that may enhance bubble-mediated scavenge and aerosolization.

511 Bubble-mediated cationic scavenge of bio-cells in clean saline water and related
512 aerosolization may contribute to global bio-matter cycling and related process of matter
513 accumulation near the ocean surface. Thus massive and long-term bubble-cationic-rotational
514 processing of matter in the oceanic water and in droplets suspended in the troposphere may
515 likely incepted the bio-matter evolution on the Earth.

516

517 *Acknowledgements.* Diatom strains have been isolated within the frame of Maestro Research
518 Grant 2012/04/A/ST10/00544 funded by National Science Centre in Cracow, Poland.

519

520 **References**

521 Aller J.Y., Kuznetsova M.R., Jahns C.J., Kemp P.F. (2005) The sea surface microlayer as a source of
522 viral and bacterial enrichment in marine aerosol. *Journal of Aerosol Science*, 36, 801-812.

523

524 Bigg E. K., Leck C. (2008) The composition of fragments of bubbles bursting at the ocean surface.
525 *Journal of Geophysical Research*, 113, D11209.

526

527 Blanchard D.C., Woodcock, A.H. (1957) Bubble formation and modification in the sea and its
528 meteorological significance. *Tellus*, 9, 145-158.

529

530 Blanchard D.C. (1963) Electrification of the atmosphere by particles from bubbles in the sea. *Progress*
531 *in Oceanography*, 1, 73-197.

532

533 Blanchard D.C., Syzdek L.D. (1970) Mechanism for the water-to-air transfer and concentration of
534 bacteria. *Science*, 170, 626-628.

535

536 Blanchard D.C., Syzdek L.D. (1978) Seven problems in bubble and jet drop researches. *Limnology*
537 *and Oceanography*, 23(3), 389-400.

538

539 Blanchard D.C., Syzdek L.D. (1982) Water-to-air transfer and enrichment of bacteria in drops from
540 bursting bubbles. *Applied and Environmental Microbiology*, 43, 1001-1005.

541

542 Blanchard D.C. (1989) The size and height to which jet drops are ejected from bursting bubbles in
543 seawater. *Journal of Geophysical Research*, 94, C8, 10,999-11,002

544

545 Budgeon A.L., Roberts D., Gasparon M., Adams N. (2012) Direct evidence of aeolian deposition of
546 marine diatoms to an ice sheet. *Antarctic Science*, 24, 527–35.

547



- 548 Burrows S.M., Elbert W., Lawrence M.G., Pöschl U. (2009) Bacteria in the global atmosphere- Part1:
549 Review and synthesis of literature data for different ecosystems. *Atmospheric Chemistry and*
550 *Physics Discussions*, 9, 10777-10827.
551
- 552 Callaghan A., de Leeuw, G., Cohen, L. (2007) Observations of Oceanic Whitecaps coverage in the
553 North Atlantic during Gale Force Winds in: *Nucleation and Atmospheric Aerosols*, Eds., D.
554 Colin, 1088-1092.
555
- 556 Czerski H., Twardowski M., Zhang X., Vagle S. (2011) Resolving size distributions of bubbles with
557 radii less than 30 mm with optical and acoustical methods, *Journal of Geophysical Research*,
558 116, C00H11, doi:10.1029/2011JC007177.
559
- 560 Duce R.A. (2001) Atmospheric input of pollutants. *Encyclopedia of Ocean Sciences*, Academic Press,
561 New York, 192-201.
562
- 563 Garbalewski C., Marks R. (1987) Latitudinal characteristics of aerosol distribution in the near surface
564 air over the Atlantic. *Acta Geophys. Pol.*, 35, 1, 77-86.
565
- 566 Gottenbos B., Grijpma D.W., van der Mei H.C., Feijen J., Busschers H.J. (2001) Antimicrobial effects
567 of positively charged surfaces on adhering Gram-positive and Gram-negative bacteria. *Journal*
568 *of Antimicrobial Chemotherapy*, 48, 7-13.
569
- 570 Katsaros K., Buettner K.J.K. (1969) Influence of Rainfall on Temperature and Salinity of the Ocean
571 Surface. *Journal of Applied Meteorology*, 8, 15-18.
572
- 573 Kropman M.F., Bakker H.J. (2001) Dynamics of water molecules in aqueous solvation shells. *Science*,
574 291, (5511), 2118-21120.
575
- 576 Liss P.S. (1983) Gas transfer: experiments and geochemical implications. In: *Air-Sea Exchange of*
577 *Gases and Particles*, Edited by Liss P.S., Slinn W.G.N., Reidel D., Dordrecht, 241-298.
578
- 579 Lovett R.F. (1978) Quantitative measurements of airborne sea salt in the North Atlantic. *Tellus*, 30,
580 350—364.
581
- 582 Marks R. (1987) Marine aerosols and whitecaps in the North Atlantic and Greenland Sea regions.
583 *Deutsche Hydrographische Zeitschrift*, 40. H.2., 71-79.
584
- 585 Marks R. (1990) Preliminary Investigations on the Influence of Rain on the Production, Concentration,
586 and Vertical Distribution of Sea Salt Aerosol. *Journal of Geophysical Research*. Vol. 95, NO.
587 C12, p. 22,299-22,304.
588
- 589 Marks R., Beldowska M. (2001) Air-Sea Exchange of Mercury Vapour over the Gulf of Gdańsk and
590 southern Baltic Sea. *Journal of Marine Systems*, 27(4), 315-324.
591
- 592 Marks R., Krucalak K., Jankowska K., Michalska M. (2001) Bacteria and Fungi in Air over the Gulf
593 of Gdańsk and Baltic Sea. *Journal of Aerosol Science*, 32(2), 43-56.
594
595
- 596 Marks, R. (2008). Dissolved oxygen supersaturation and bubble formation in the southern Baltic Sea
597 coastal waters. *Hydrology Research*, 39 (3), 229-236.
598
- 599 Marks R. (2014) Bubble Rotational Features – Preliminary Investigations. *Oceanography: Open*
600 *Access*, 2: 128, doi: 10.4172/2332-2632.1000128.
601



- 602 Marks R. (2015) Sub-bubble Bi-pirouette Splicing of Cationic and Anionic Bases as a Process of
603 RNA/DNA Creation. *Oceanography: Open Access*, 2: 128, doi: 10.4172/2332-2632.1000135.
604
- 605 Matthais-Maser S., Jaenicke R. (1994) Examination of atmospheric bioaerosol particles with radii >
606 0.2 μm . *Journal of Aerosol Science*, 25, 1605-1613.
607
- 608 Mayol E., Jiménez M.A. Herndl G.J., Duarte C.M., Arrieta J.M. (2014) Resolving the abundance and
609 air-fluxes of airborne microorganisms in the North Atlantic Ocean. *Frontiers in Microbiology*,
610 5, Articles 557, 1-9.
611
- 612 Monahan E.C., Fairall C.W., Davidson K.L., Boyle P.J. (1983) Observed interrelationships between
613 10 m winds, ocean whitecaps and marine aerosols. *Quarterly Journal of the Royal*
614 *Meteorological Society*, 109, 379-392.
615
- 616 Novakov T., Penner J. (1993) Large contribution of organic aerosols to cloud-condensation-nuclei
617 concentrations. *Nature*, 365, 823-826.
618
- 619 Sherilyn C., Fritz S.C., Brinson B.E., Billups W.E., Lonnie G., Thompson L.G. (2015) Diatoms at
620 >5000 meters in the Quelccaya Summit Dome Glacier, Peru. *Arctic, Antarctic, and Alpine*
621 *Research*, 47(2), 369–374.
622
- 623 Stanish L.F., Bagshaw E.A., McKnight D.M., Fountain A.G., Tranter M. (2013) Environmental
624 factors influencing diatom communities in Antarctic cryoconite holes. *Environmental Research*
625 *Letters*, 8, 045006 (8pp) doi:10.1088/1748-9326/8/4/045006.
626
- 627 Stramska M., Marks R., Monahan E. C. (1990) Bubble-mediated aerosol production as a consequence
628 of wave breaking in supersaturated (hyperoxic) seawater. *Journal of Geophysical Research*, 95,
629 18,281-18,288.
630
- 631 Stramski D., Tęgowski J. (2001) Effects of intermittent entrainment of air bubbles by breaking wind
632 waves on ocean reflectance and underwater light field, *Journal of Geophysical*
633 *Research*, 106(C12), 31,345–31,360, doi: 10.1029/2000JC000461.
634
- 635 Terray E.A., Donelan M.A., Agarwal Y.C., Drennan, W.M., Kahma K. K., Williams III A.J., Hwang
636 P.A., Kitajgorodskii, S.A. (1996) Estimates of kinetic energy dissipated under breaking waves.
637 *Journal of Physical Oceanography*, 26, 792-807.
638
- 639 Thorpe S.A. (2001) Breaking waves and near-surface turbulence. In: *Encyclopedia of Ocean Sciences*,
640 Steele J.H., Thorpe S.A. Turekian, K.K. (eds.) . San Diego, USA, Academic Press, 349-351.
641
- 642 Tuck A. (2002) The role of atmospheric aerosols in the origin of life. *Surveys in Geophysics*, 23, 379-
643 409.
644
- 645 Witkowski A., Kociołek J.P., Compère P. (eds) (2012) Diatom Taxonomy and ecology. From local
646 discoveries to global impacts. *Lange-Bertalot Festschrift. Nova Hedwiga Beihefte*, 141, 1-540.
647
- 648 Woodcock A. (1953) Salt nuclei in the marine air as a function of altitude and wind force. *Journal of*
649 *Meteorology*, 10, 362-371.
650
- 651 Woolf D. K. (1997) Bubbles and their role in gas exchange, *The Sea Surface and Global Change*, Eds.
652 P.S. Liss, R.A. Duce, Cambridge University Press, 173-205.
653
- 654 Woolf D.K., Thorpe S.A. (1991) Bubbles and the air-sea exchange of gases in near saturation
655 conditions. *Journal of Marine Research*, 49, 435-466.
656



- 657 Weber M.E., Blanchard D.C., Syzdek L.D. (1983) The mechanism of scavenging of waterborne
658 bacteria by a rising bubble. *Limnology and Oceanography*, 28(1), 101-105.
659
660 Yu L. (2007) Global Variations in Oceanic Evaporation (1958–2005): The Role of the Changing Wind
661 Speed. *Journal of Climate*, 20, 5376–5390.